# Image Charges Re-Imagined

H Alshal[1,2]*; T Curtright[2]†; and S Subedi[2]‡
[1]Department of Physics, Cairo University, Giza, 12613, Egypt
[2]Department of Physics, University of Miami, Coral Gables, FL 33124-8046, USA

21 August 2018

"Few things are harder to put up with than the annoyance of a good example." - Mark Twain

**Abstract**

We discuss the grounded, equipotential ellipse in two-dimensional electrostatics to illustrate different ways of extending the domain of the potential and placing image charges such that boundary conditions are satisfied. In particular, we compare and contrast the Kelvin and Sommerfeld image methods.

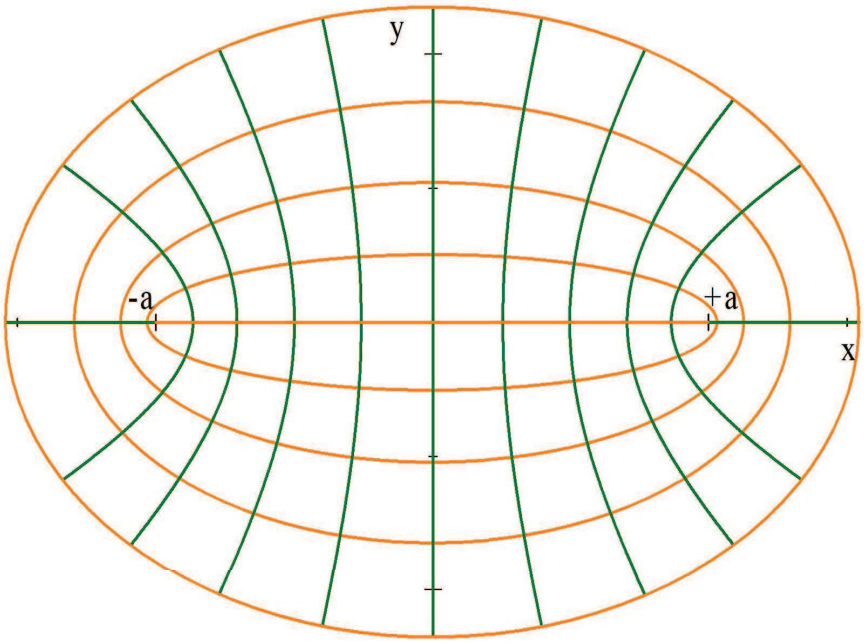


*halshal@sci.cu.edu.eg
†curtright@miami.edu
‡sushil.subedi04@gmail.com

## Introduction

When a source charge is placed near a real, grounded conductor, electrical charge flows between the ground and the conductor. In the static limit, for an idealized conductor, the resulting induced charge distribution is entirely on the surface of the conductor. In this ideal static situation the *interior* of the conductor is an equipotential containing no charge, and therefore not very interesting. However, for mathematical expediency, in some cases one can easily *imagine* a distribution of charge located entirely *inside* the conductor, instead of on the surface, which gives exactly the same *exterior* effects as the actual surface charge distribution.

All this is well-known, of course, but it may not be fully appreciated that the imagined distribution of charge within the conductor is *not* uniquely determined. Perhaps the most interesting aspect of this non-uniqueness lies in the mathematical freedom to choose the interior of an idealized conductor (i.e. the domain of the image charge and its potential) as an extension of the exterior (i.e. the domain of the real source charge and its potential) to be almost *any* imagined manifold, with the only essential restriction being that the image and source domains have in common a boundary, namely, the surface of the ideal conductor.[1]

This somewhat surprising mathematical freedom can be illustrated by a simple example to be discussed below: The grounded two-dimensional ellipse. Two image methods, established long ago by Thomson (a.k.a. Lord Kelvin) [12] and somewhat later by Sommerfeld [11], will be compared and contrasted. The image domains for these two methods have different geometries, but nevertheless give exactly the same physical results. The Kelvin method has the advantage that the Green function [9] is usually easier to extend from the source domain to the image domain. On the other hand, the Sommerfeld method has the advantage that the location of the image is always obvious given the location of the actual source charge.

## Green Functions for a 2D Ellipse

This problem is nicely solved using complex analysis, as has been known since the 19th century (e.g. see the literature cited in [7]). However, here we use real variables in anticipation of higher dimensional situations. (An Appendix provides the relation between our choice of real variables and those of the conventional complex plane.) In terms of real elliptic coordinates for the $xy$-plane[2] as shown in the title page Figure,

$$x = a\cosh u\cos v\ , \quad y = a\sinh u\sin v\ , \quad 0 \le u \le \infty\ , \quad 0 \le v \le 2\pi\ , \tag{1}$$

the standard 2D Laplacian Green function on the plane is given by

$$G\left(u_1, v_1; u_2, v_2\right) = -\frac{1}{4\pi}\left|u_1 - u_2\right| - \frac{1}{4\pi}\ln\left(1 + e^{-2|u_1-u_2|} - 2e^{-|u_1-u_2|}\cos\left(v_1 - v_2\right)\right)\ . \tag{2}$$

Note that in addition to being $2\pi$-periodic in each of the $v$s, this Green function is totally symmetric: $G\left(u_1, v_1; u_2, v_2\right) = G\left(u_2, v_2; u_1, v_1\right)$. By construction, $G$ is a fundamental solution of the equation

$$\left(\frac{\partial^2}{\partial u_1^2} + \frac{\partial^2}{\partial v_1^2}\right) G\left(u_1, v_1; u_2, v_2\right) = -\ \delta\left(u_1 - u_2\right)\ \delta\left(v_1 - v_2\right)\ , \tag{3}$$

and it incorporates some implicit boundary conditions. For example, all $v$ dependence in $G$ is exponentially suppressed as either $u_1$ or $u_2$ become infinite, with the other $u$ fixed.

### The Kelvin image method

Characterized generally, albeit rather vaguely, the Kelvin image method makes use of both the interior *and* the exterior of the ellipse, placing source and image charges in opposite regions so as to satisfy boundary conditions. In this framework, an obvious construction of a Green function for a grounded ellipse is given by the linear combination

$$G_o\left(u_1, v_1; u_2, v_2\right) = G\left(u_1, v_1; u_2, v_2\right) - G\left(u_1, v_1; 2U - u_2, v_2\right) \tag{4}$$

[1] The topology of the extended manifold may also be restricted, but here we will not discuss that issue in any explicit detail.

[2] The straight line segment connecting the two elliptical foci on the $x$-axis at $\pm a$ is covered twice using real elliptic coordinates.

where the grounded ellipse consists of points given by $(U, v)$ for a fixed $U$ and $0 \leq v \leq 2\pi$. By construction, $G_o\,(u_1, v_1; U, v_2) = 0$ for all $v_2$. From the symmetry of $G$ it is also true that $G_o\,(U, v_1; u_2, v_2) = 0$ for all $v_1$. For a general distribution of source charge either inside or outside the grounded ellipse, as given by $\rho\,(u, v)$, the solution of

$$\left(\frac{\partial^2}{\partial u^2} + \frac{\partial^2}{\partial v^2}\right) \Phi\,(u, v) = -k\ \rho\,(u, v) \tag{5}$$

is then reduced to the evaluation of an integral involving $G_o$ and $\rho$. In particular, for field points and actual sources outside the grounded ellipse, the electric potential is

$$\Phi\,(u_1, v_1) = k \int_{U<u_2\leq\infty} \int_{0\leq v_2\leq 2\pi} G_o\,(u_1, v_1; u_2, v_2)\,\rho\,(u_2, v_2)\,du_2 dv_2\ . \tag{6}$$

Here $k$ is a 2D analogue of the Coulomb constant.

The first $G$ in (4) is universally interpreted as the potential at field point $(u_1, v_1)$ produced by a positive unit point source at location $(u_2, v_2)$. The second $G$ in (4) is similarly interpreted as the potential at field point $(u_1, v_1)$ produced by another point-like, but in this case negative, *Kelvin image* at location $(2U - u_2, v_2)$. However, for the grounded ellipse construction in (4) there are some interesting — perhaps unexpected — features.

For both field and source points inside the grounded ellipse, such that $0 \leq u_1, u_2 \leq U$, the Kelvin image is always outside that ellipse with $U \leq 2U - u_2 \leq 2U$, and therefore the image is *never* located at infinity[3] as long as both $a \neq 0$ and $U \neq \infty$. That is to say, to implement an interior Green function construction inside a grounded ellipse at $u = U$, it suffices to use a single point-like Kelvin image that lies between the confocal ellipses at $u = U$ and $u = 2U$. As expected, the image is outside the source domain defined by $0 \leq u \leq U$. In any case, only *one* copy of the plane $\mathbb{E}_2$ is sufficient for the construction of the interior Green function.

On the other hand, for field and source points outside the grounded ellipse, such that $U \leq u_1, u_2 \leq \infty$, the Kelvin image is inside that ellipse, with $0 \leq 2U - u_2 \leq U$, only so long as the source is not too distant from the grounded ellipse. That is to say, the interior of the original grounded ellipse contains the image only for $u_2 \leq 2U$. But if the source is more distant, with $u_2 > 2U$, the chosen Kelvin image of the point source passes through the line connecting the two foci and moves onto a *second* copy of $\mathbb{E}_2$ as also defined by (1) except with negative $u$. Therefore, for the point-like Kelvin image construction of the complete exterior Green function as expressed in (4), *two* copies of the real plane are required: One for $u > 0$ and another for $u < 0$. Effectively, the two elliptical foci on the $x$-axis at $x = \pm a$ are connected by a straight line segment that acts as a branch line "doorway" joining together these two copies of $\mathbb{E}_2$.

So, to solve the exterior electric potential problem for a grounded ellipse, when real coordinates are used and point-like Kelvin images are located in an obvious way, a branched manifold is necessarily encountered. To put it another way, the actual, real interior of a grounded 2D elliptical conductor is insufficient to accommodate the location of a single point-like Kelvin image for an exterior point source, when that source is far from the conductor. More interior space is needed!

### Mapping an infinite cylinder onto planes

What is at work here is the fact that $G$ in (2) is really a Green function not just for the semi-infinite cylinder, with $u \geq 0$, but actually provides a solution to (3) for the infinite $uv$-cylinder, where $-\infty \leq u \leq +\infty$, along with $0 \leq v \leq 2\pi$. So no matter where the source is placed on that infinite cylinder, to construct $G_o$ such that it vanishes at a fixed value of $u$, there is always room to accommodate a Kelvin point image.

The only open issue is then how to map the infinite $uv$-cylinder onto one or more copies of the $xy$-plane. Sticking with the $x\,(u, v)$ and $y\,(u, v)$ relations in (1) gives a map that produces two copies of $\mathbb{E}_2$ as represented by the embedding shown in Figure 1[4] for the case $U = 3/2$. The original infinite $uv$-cylinder

[3] This differs from a grounded circle in 2D (or sphere in 3D) where the image is located by inversion and *can* move toward infinity as the source moves toward the center of the circle (or sphere). The limit where the ellipse becomes a circle of radius $R$ is achieved here by $R = \lim_{a\to 0} [a \cosh U|_{U=\ln(2R/a)} = \lim_{a\to 0} [a \sinh U|_{U=\ln(2R/a)}$. In this limit, only one copy of $\mathbb{E}_2$ is sufficient to solve either the interior or the exterior problem using the Kelvin method. See [2] for a thorough discussion of the grounded circular ring in 2D, where the standard Kelvin method is compared to the Sommerfeld method in considerable detail.

[4] For the chosen 3D embedding the surface has the appearance of being intrinsically curved, but that is an artefact of the parameterization. That part of the surface either above or below the blue line in Figure 1 corresponds to an open subset of $\mathbb{E}_2$.

is flared out by the map onto $x$ and $y$, both for large positive and for large negative $u$, but pinched down to a straight line segment connecting the foci at $x = \pm a$ when $u = 0$, with that segment situated "below" the grounded ellipse at $u = U$ ($= 3/2$ in the Figure). This is the geometry that underlies the Kelvin image method as applied here. The pinched line segment has some obviously singular geometric features, but these are not pathological.

On the other hand, there is another clear choice to map the infinite $uv$-cylinder onto planes that gives a different geometry. Rather than pinch the cylinder shut in terms of $x$ and $y$, at $u = 0$ or some other value of $u$, the cylinder may be folded around the location of the grounded ellipse so that the submanifold below the fold is just a "mirror image" of the submanifold above the fold. (Please see Figure 2.[5]) This leads to the Sommerfeld image method which we describe in detail in the following. The fold also has some obviously singular geometric features, but again these are not pathological.

**The Sommerfeld image method**

Consider the same exterior Green function situation using Sommerfeld images. (The history of this alternate method is discussed in [8].) In this approach, the interior of the ellipse is eliminated, and two copies of the plane outside the grounded ellipse are joined together along the grounded ellipse.

The new parameterization of both copies of the $xy$-plane outside the ellipse with $u = U > 0$, again written in terms of real elliptic coordinates, is[6]

$$u = U + |w| \ , \tag{7}$$

$$x = a\cosh\left(U + |w|\right)\cos v \ , \quad y = a\sinh\left(U + |w|\right)\sin v \ , \quad -\infty \le w \le \infty \ , \quad 0 \le v \le 2\pi \ . \tag{8}$$

So, when both field and source points are on the upper branch of the surface, such that $0 < w_1, w_2 < \infty$, the Green function is

$$G\left(w_1, v_1; w_2, v_2\right) = -\frac{1}{4\pi}\left|w_1 - w_2\right| - \frac{1}{4\pi}\ln\left(1 + e^{-2|w_1 - w_2|} - 2e^{-|w_1 - w_2|}\cos\left(v_1 - v_2\right)\right) \ . \tag{9}$$

But when the field point is on the upper branch and the source is on the lower branch, albeit with the same convention $0 < w_1, w_2 < \infty$, the Green function is

$$G\left(w_1, v_1; -w_2, v_2\right) = -\frac{1}{4\pi}\left(w_1 + w_2\right) - \frac{1}{4\pi}\ln\left(1 + e^{-2(w_1 + w_2)} - 2e^{-(w_1 + w_2)}\cos\left(v_1 - v_2\right)\right) \ . \tag{10}$$

In this approach the exterior Green function for a grounded ellipse is the linear combination

$$\begin{aligned} G_o\left(w_1, v_1; w_2, v_2\right) &= G\left(w_1, v_1; w_2, v_2\right) - G\left(w_1, v_1; -w_2, v_2\right) \\ &= -\frac{1}{4\pi}\left|w_1 - w_2\right| + \frac{1}{4\pi}\left(w_1 + w_2\right) - \frac{1}{4\pi}\ln\left(1 + e^{-2|w_1 - w_2|} - 2e^{-|w_1 - w_2|}\cos\left(v_1 - v_2\right)\right) \\ &\quad + \frac{1}{4\pi}\ln\left(1 + e^{-2(w_1 + w_2)} - 2e^{-(w_1 + w_2)}\cos\left(v_1 - v_2\right)\right) \ , \end{aligned} \tag{11}$$

assuming that both field and source points are on the upper branch, i.e. $0 \le w_1, w_2 \le \infty$. Otherwise, $G\left(w_1, v_1; w_2, v_2\right) = G\left(w_2, v_2; w_1, v_1\right)$ and $G_o\left(-w_1, v_1; w_2, v_2\right) = -G_o\left(w_1, v_1; w_2, v_2\right)$.

Remarkably, as the reader may readily verify, the expressions (4) and (11) give exactly the same functions on the $xy$-plane when both field point $(x_1, y_1)$ and source point $(x_2, y_2)$ are located outside the grounded ellipse and on the upper $\mathbb{E}_2$ branch, despite the differences in the Kelvin and Sommerfeld image locations as evident upon comparing Figure 1 with the following Figure 2.

[5] As in the previous Figure, for the chosen 3D embedding the surface has the appearance of being intrinsically curved, but that is again an artefact of the parameterization. That part of the surface either above or below the red ellipse in Figure 2 corresponds to an open subset of $\mathbb{E}_2$.

[6] If the apparent $du/dw$ slope discontinuity causes anxiety on the part of the reader, one may take instead $u\left(w\right) = \left(U^{2p} + w^{2p}\right)^{1/2p}$ for $p > 1/2$, again with $-\infty \le w \le \infty$. For example, see [2]. However, the ensuing complications in expressions involving Green functions are not worth making this generalization, in our opinion.

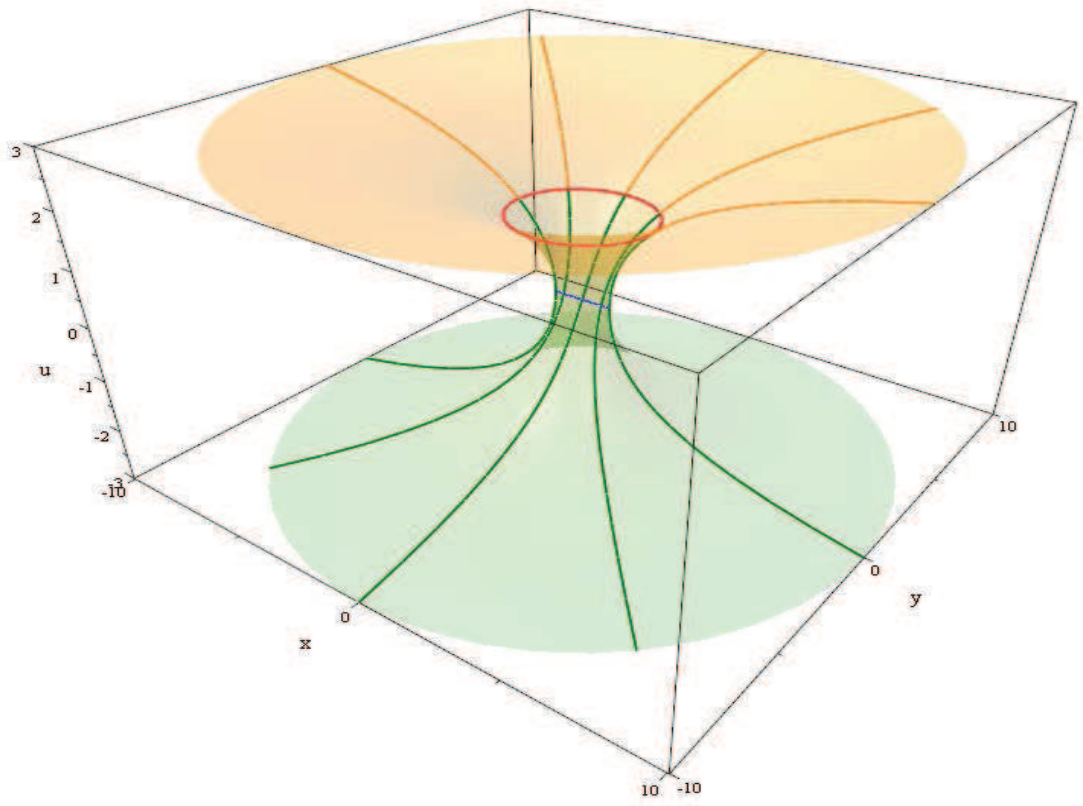


Figure 1: Representative "trajectories" for exterior sources (orange) and their Kelvin images (green) for a grounded ellipse (red) with $U = 3/2$. As a point source moves away from the red ellipse along one of the orange curves, its image moves away from the red ellipse along a corresponding (connected) green curve. A straight line segment between the foci is shown in blue.

Visualization of the features in these 3D Figures — especially their differences — may be easier if 2D vertical slices are considered. In Figure 3, the source and image domains along the $y$-axis are shown in green for the Kelvin method and in orange for the Sommerfeld method. Particular choices for point sources and their images are shown as small circles, squares, or diamonds, for an ellipse whose $x = 0$ points are shown in red. The source domain is always the same — namely, the planar region outside the grounded ellipse — no matter what image method is under consideration, so the orange and green curves in the Figure are the same for $u > 3/2$ or $w > 0$.

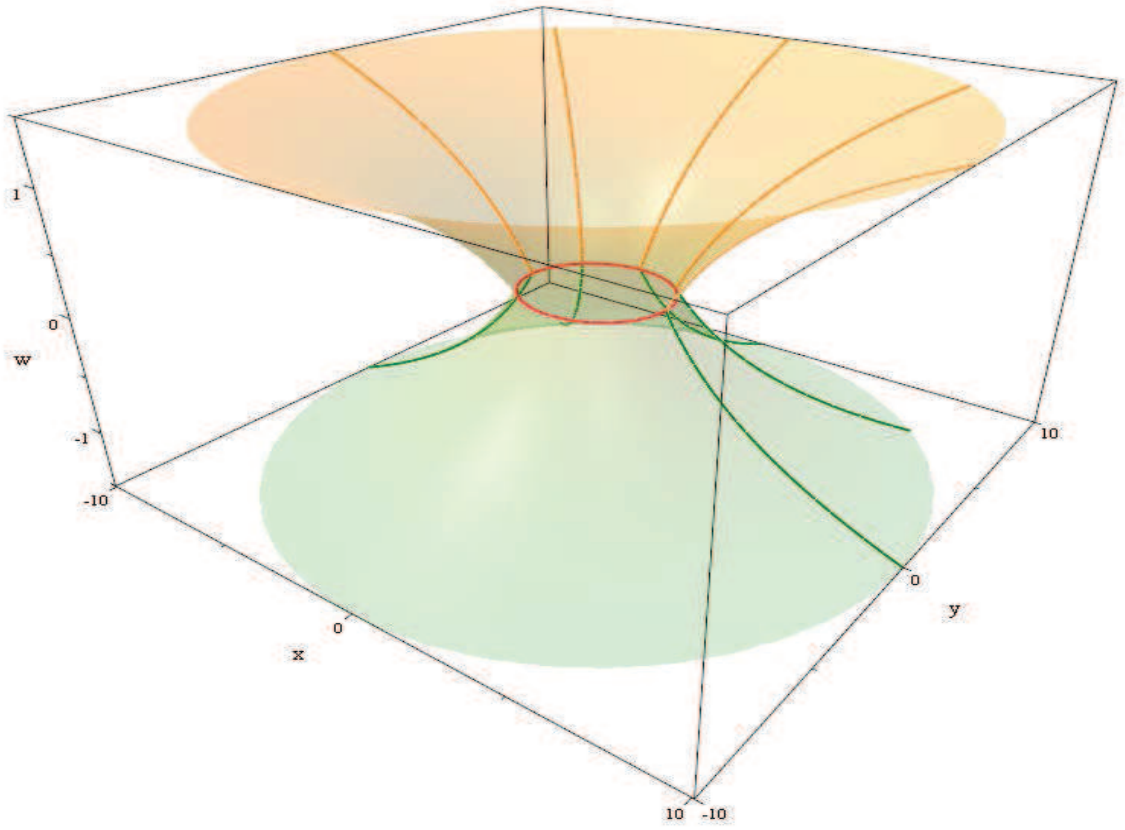


Figure 2: Representative trajectories for exterior sources (orange) and their Sommerfeld images (green) for a grounded ellipse (red), again with $U = 3/2$. All $(x, y)$ points inside the red ellipse are excluded from the 2D manifold in this method.

In Figure 4, the source and image domains along the $x$-axis are shown in green for the Kelvin method and in orange for the Sommerfeld method. As before, particular choices for point sources and their images are shown as small circles, squares, or diamonds, and the $y = 0$ points on the ellipse are shown in red. Once again, the source domain is always the same no matter what image method is under consideration, but the image domains differ, depending on how the manifold is extended beyond the source domain.

All things considered, it seems fair to say the image domain is largely determined just by one's imagination.

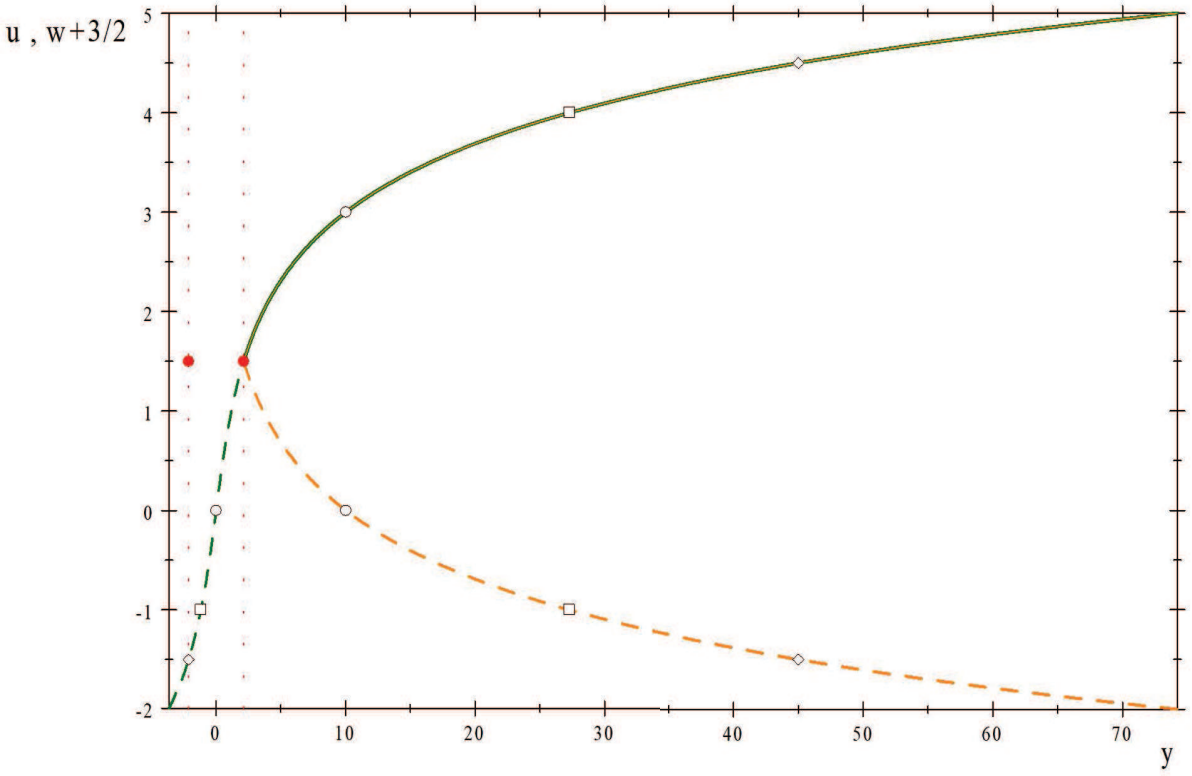


Figure 3: Source and image domains for $x = 0$, as solid and dashed curves, respectively.

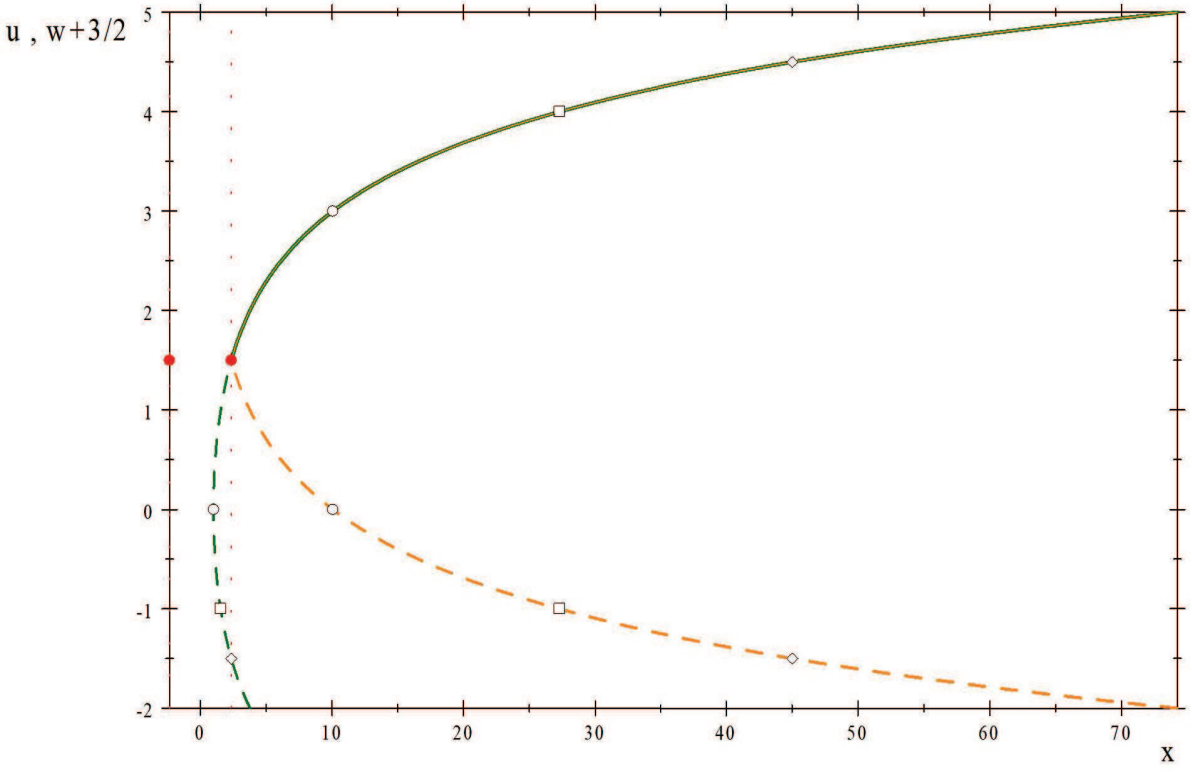


Figure 4: Source and image domains for $y = 0$, as solid and dashed curves, respectively.

## Induced Charge Density

The actual linear charge density induced on the grounded ellipse is proportional to the normal component of the electric field evaluated in the limit where the field point approaches the ellipse. It suffices to consider the density induced by a unit point source outside the ellipse. Then the relevant normal electric field is just $-\partial G_o/\partial u_1|_{u_1=U}$ for the Kelvin image method, or $-\partial G_o/\partial w_1|_{w_1=0}$ for the Sommerfeld image method. The results are the same, using either method. The situation of interest for the external problem involves a unit source at $u_2 > U$ or $w_2 > 0$.

In terms of the result for the Sommerfeld method, (11), we find the linear charge density

$$\lambda\left(v_1; w_2, v_2\right) = -\left.\frac{\partial}{\partial w_1} G_o\left(w_1, v_1; w_2, v_2\right)\right|_{w_1=0,\ w_2>0} = \frac{1}{2\pi}\frac{e^{-2w_2}-1}{e^{-2w_2}-2e^{-w_2}\cos\left(v_1-v_2\right)+1} \ . \tag{12}$$

Note that the total charge induced by a $+1$ source is always $-1$,

$$\int_0^{2\pi} \lambda\left(v_1; w_2, v_2\right) dv_1 = -1 \ , \tag{13}$$

even if the unit source is removed to infinity.[7] In that infinite limit, the induced charge density becomes constant around the ellipse.

$$\lambda\left(v_1; w_2, v_2\right) \underset{w_2\to\infty}{\sim} -\frac{1}{2\pi} \ . \tag{14}$$

Plots of the charge density for various selected source distances from the grounded ellipse are straightforward to produce and evince all the expected features when expressed in terms of our chosen elliptic coordinates.

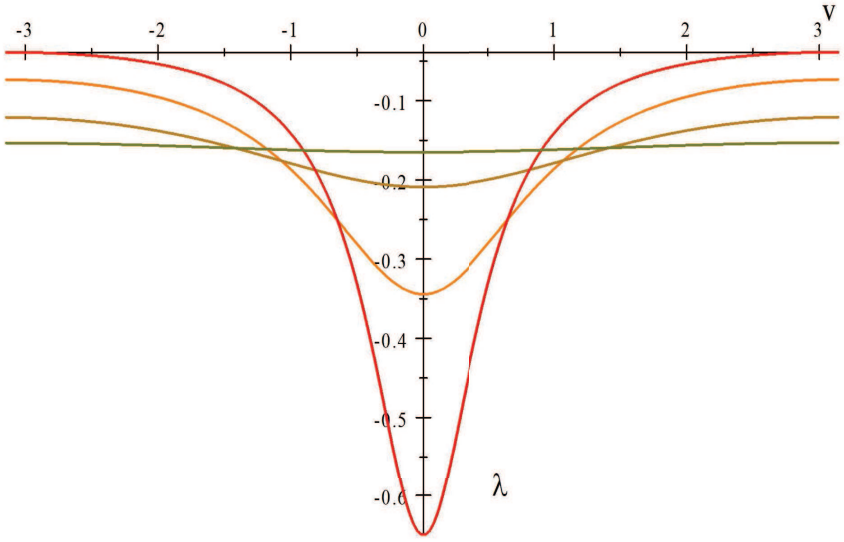


Figure 5: $\lambda$ as a function of $v = v_1 - v_2$ for various $w_2$. Specifically, $w_2 = 1/2$ red, $w_2 = 1$ orange, $w_2 = 2$ sienna, $w_2 = 4$ brown.

[7] This is a peculiarity of the long-range Coulomb potential in 2D — it's logarithmic! In 3D the charge induced on a grounded ellipsoid by a unit source outside the sphere is not always $-1$, and in fact falls to zero as the source is removed to infinity [4, 14]. For a grounded hyper-sphere in $N$ spatial dimensions, it is an interesting exercise to show the induced charge falls as a function of the source distance like $r^{2-N}$ [1].

## The Straight Line

A straight line limit of the ellipse is achieved by first setting $v = \pi/2$ in (1) so that $x \equiv 0$, and then letting $a \to \infty$ and $u \to 0$ so that $\lim_{a\to\infty, u\to 0} (a \sinh u) = y$ remains finite. The essential idea is that as $a \to \infty$ the elliptical $(u, v)$ coordinates near the center of the $x$-axis become just rectangular Cartesian coordinates, $(x, y)$. This behavior is evident in the title page Figure, even for finite $a$.

That is to say, let $u = y/a$ as $a \to \infty$ so that

$$a \sinh u \to ay/a = y \ . \tag{15}$$

At the same time, let $U = Y/a$ for $v = \pi/2$. Then $y(U, \pi/2) \to Y$ as $a \to \infty$. In this limit the Green functions (2) and (4) for similarly restricted $u$s and $v$s are given by

$$\begin{aligned} G(u_1 = y_1/a, v_1 = \pi/2; u_2 = y_2/a, v_2 = \pi/2) &= -\frac{1}{4\pi a}|y_1 - y_2| - \frac{1}{4\pi}\ln\left(1 + e^{-2|y_1-y_2|/a} - 2e^{-|y_1-y_2|/a}\right) \\ &\underset{a\to\infty}{\sim} -\frac{1}{2\pi}\ln(|y_1 - y_2|/a) + O\left(\frac{1}{a}\right) \ , \end{aligned} \tag{16}$$

$$G_o(u_1 = y_1/a, v_1 = \pi/2; u_2 = y_2/a, v_2 = \pi/2) \underset{a\to\infty}{\sim} -\frac{1}{2\pi}\ln\left(\frac{|y_1 - y_2|}{|y_1 - 2Y + y_2|}\right) + O\left(\frac{1}{a}\right) \ . \tag{17}$$

Finally then,

$$\lim_{a\to\infty} G_o(u_1 = y_1/a, v_1 = \pi/2; u_2 = y_2/a, v_2 = \pi/2) = -\frac{1}{2\pi}\ln\left(\frac{|y_1 - y_2|}{|y_1 + y_2 - 2Y|}\right) \ . \tag{18}$$

But for $y_1 > Y$ and $y_2 > Y$, this is precisely the 2D Green function at field point $(0, y_1)$ for a grounded straight line parallel to the $x$-axis, passing through the point $(x, y) = (0, Y)$, as obtained by placing at the point $(0, 2Y - y_2)$ a single negative Kelvin point image of a unit point source placed at position $(0, y_2)$. Of course, in this straight line limit where $x_1 = x_2$ the system is translationally invariant with respect to $x$, so there is no $x$ dependence in the final Green functions.

When $x_1 \neq x_2$ but both are fixed and small, while $a$ becomes infinite, a similar but slightly more tedious limit calculation gives the 2D Green function on the grounded half-plane, namely,

$$G_{half-plane}(x_1, y_1; x_2, y_2) = -\frac{1}{2\pi}\ln\left(\frac{\sqrt{(x_1 - x_2)^2 + (y_1 - y_2)^2}}{\sqrt{(x_1 - x_2)^2 + (y_1 + y_2 - 2Y)^2}}\right) \ . \tag{19}$$

Once again, translational invariance with respect to $x$ accounts for the dependence on only the difference, $x_1 - x_2$. We leave the detailed derivation of $G_{half-plane}$ from $G_o$ for the ellipse as an exercise for the reader.[8]

## Discussion

The standard problems involving a grounded circular ring in 2D [2] or grounded spheres in higher dimensions [1] can also be easily solved using either the Kelvin or Sommerfeld methods. However, there are many problems where the Kelvin method is very difficult, if not impossible, to implement, but which are directly solvable by the Sommerfeld method. Grounded semi-infinite planes and the circular disk in 3D Euclidean space provide well-studied examples [11, 10, 13, 5, 6, 7].

Beyond these previously solved examples, the grounded ellipsoid in 3D and hyper-ellipsoids in higher dimensions are difficult problems that should be more tractable using Sommerfeld images. Existing image methods applied to these problems are quite involved, and usually require detailed properties of ellipsoidal harmonics [3]. In fact, extant treatments of the exterior 3D Green function problem for grounded ellipsoids use, in addition to an interior point image, a *continuous* distribution of Kelvin image charge on the surface of an interior confocal ellipsoid [4, 14] (also see Sections 7.4.3 and 7.4.4 in [3]). This non-trivial array of image charges results from requiring that all such charges reside entirely within the physical interior of the

[8] Results given in the Appendix may be helpful.

ellipsoid, *without* invoking a second copy of $\mathbb{E}_3$. In our opinion, these treatments are tantamount to walking on broken glass while bare-footed.

In contrast, the Sommerfeld method applied to a grounded ellipsoid embedded in $N$ Euclidean dimensions only requires a single point image of the point source, in complete parallel to the grounded 2D ellipse treated here, albeit at the cost of introducing a second copy of $\mathbb{E}_N$. Therefore, in principle the Sommerfeld method should simplify the analysis required to construct Green functions for such ellipsoids, both conceptually and practically.

**Acknowledgements** It has been our pleasure to reconsider this elementary subject during the Sommerfeld Sesquicentennial year. This work was supported in part by a University of Miami Cooper Fellowship and by a Clark Way Harrison Visiting Professorship at Washington University in Saint Louis.

## Appendix: Complex Variables

Let

$$x + iy = a\,(\cos v \cosh u + i \sin v \sinh u) = a \cosh{(u + iv)} \ . \tag{A1}$$

That is to say, $u + iv = \pm \arccosh\left(\frac{x+iy}{a}\right) + 2i\pi k \mid k \in \mathbb{Z}$. Choose the + solution with $k = 0$ so that

$$u = \mathrm{Re}\left(\arccosh\left(\frac{x+iy}{a}\right)\right) \ , \quad v = \mathrm{Im}\left(\arccosh\left(\frac{x+iy}{a}\right)\right) \ . \tag{A2}$$

Then find

$$\begin{aligned} r^2 = x^2 + y^2 &= a^2\left(\cosh^2 u \ \cos^2 v + \sinh^2 u \ \sin^2 v\right) \\ &= \frac{1}{2}\ a^2\,(\cosh 2u + \cos 2v) = a^2 \arccosh\left(\frac{x+iy}{a}\right) \arccosh\left(\frac{x-iy}{a}\right) \ , \end{aligned} \tag{A3}$$

as well as

$$x^2 - y^2 = a^2\left(\cosh^2 u \ \cos^2 v - \sinh^2 u \ \sin^2 v\right) = \frac{1}{2}\ a^2\,(\cosh 2u \cos 2v + 1) \ , \tag{A4}$$

$$xy = a^2 \cosh u \ \cos v \ \sinh u \ \sin v = \frac{1}{4}\ a^2 \sinh 2u \sin 2v \ . \tag{A5}$$

In addition find

$$\begin{aligned} \sinh^2 2u &= \frac{1}{2}\ \cosh 4u - \frac{1}{2} \\ &= \frac{2}{a^4}\left(x^2 + y^2\right)^2 + \frac{2}{a^2}\left(y^2 - x^2\right) + \frac{2}{a^4}\left(x^2 + y^2\right)\sqrt{\left((x-a)^2 + y^2\right)\left((x+a)^2 + y^2\right)} \ , \end{aligned} \tag{A6}$$

along with

$$v = \arccos\left(\frac{x/a}{\cosh u}\right) = \arcsin\left(\frac{y/a}{\sinh u}\right) \ . \tag{A7}$$

# References


[1] H Alshal and T Curtright, "Grounded Hyperspheres as Squashed Wormholes" arXiv:1806.03762 [physics.class-ph].

[2] T Curtright, H Alshal, P Baral, S Huang, J Liu, K Tamang, X Zhang, and Y Zhang. "The Conducting Ring Viewed as a Wormhole" arXiv:1805.11147 [physics.class-ph].

[3] G Dassios, *Ellipsoidal Harmonics*, Cambridge University Press (2013) ISBN-13: 978-0521113090.

[4] G Dassios, "Directional dependent Green's function and Kelvin images" Arch. Appl. Mech. 82 (2012) 1325–1335.

[5] L C Davis and J R Reitz, "Solution to potential problems near a conducting semi-infinite sheet or conducting disc" Am. J. Phys. 39 (1971) 1255-1265.

[6] L C Davis and J R Reitz, "Solution of potential problems near the corner of a conductor" J. Math. Phys. 16 (1975) 1219–1226.

[7] D G Duffy, *Green's Functions with Applications*, Second Edition, CRC Press (2017) ISBN-13: 978-1482251029.

[8] M Eckert, *Arnold Sommerfeld: Science, Life and Turbulent Times 1868-1951*, Springer-Verlag (2013) ISBN-13: 978-1461474609.

[9] G Green, *An Essay on the Application of Mathematical Analysis to the Theories of Electricity and Magnetism*, Nottingham (1828).

[10] E W Hobson, "On Green's function for a circular disc, with application to electrostatic problems" Trans. Cambridge Philos. Soc. 18 (1900) 277- 291.

[11] A Sommerfeld, "Über verzweigte Potentiale im Raum" Proc. London Math. Soc. (1896) s1-28 (1): 395-429; ibid. 30 (1899) 161.

[12] W Thomson and P G Tait, *Treatise on Natural Philosophy*, Part I & Part II, Cambridge University Press (1879 & 1883).

[13] L Waldmann, "Zwei Anwendungen der Sommerfeld'schen Methode der verzweigten Potentiale" Physikalische Zeitscrift 38 (1937) 654–663

[14] C Xue and S Deng, "Green's function and image system for the Laplace operator in the prolate spheroidal geometry" AIP Advances 7 (2017) 015024.